

Discretisation effects and the influence of walking speed in cellular automata models for pedestrian dynamics

Ansgar Kirchner^{1,2,‡}, Hubert Klüpfel^{2,3}, Katsuhiro Nishinari^{4,1},
Andreas Schadschneider¹, Michael Schreckenberg²

¹ Institut für Theoretische Physik, Universität zu Köln, 50923 Köln, Germany

² Physik von Transport und Verkehr, Universität Duisburg-Essen, 47048 Duisburg, Germany

³ TraffGo GmbH, Falkstr. 73-77, 47058 Duisburg, Germany

⁴ Department of Applied Mathematics and Informatics, Ryukoku University, Shiga, Japan

E-mail: aki@thp.uni-koeln.de, kluepfel@traffgo.com,
knishi@rins.ryukoku.ac.jp, as@thp.uni-koeln.de,
schreckenberg@uni-duisburg.de

Abstract. We study discretisation effects in cellular automata models for pedestrian dynamics by reducing the cell size. Then a particle occupies more than one cell which leads to subtle effects in the dynamics, e.g. non-local conflict situations. Results from computer simulations of the floor field model are compared with empirical findings. Furthermore the influence of increasing the maximal walking speed v_{\max} is investigated by increasing the interaction range beyond nearest neighbour interactions. The extension of the model to $v_{\max} > 1$ turns out to be a severe challenge which can be solved in different ways. Four major variants are discussed that take into account different dynamical aspects. The variation of v_{\max} has strong influence on the shape of the flow-density relation. We show that walking speeds $v_{\max} > 1$ lead to results which are in very good agreement with empirical data.

PACS numbers: 45.70.Vn, 02.50.Ey, 05.40.-a

Submitted to: *JSTAT*

1. Introduction

The understanding of the dynamical features of pedestrian dynamics has been the aim of many investigations over the last years [1, 2, 3]. Recently also approaches based on cellular automata (CA) have been suggested. CA models are discrete in space, time and state variables. On the one hand, this makes the models ideally suited

‡ Present address: BERATA GmbH, Geschäftsstelle Hamburg, Nagelsweg 24, 20097 Hamburg

for large-scale computer simulations. On the other hand, the discreteness has to be regarded as an approximation of reality. In this paper we want to investigate some more fundamental questions related to general aspects of physical modelling using discrete models. More specifically, we try to elucidate the qualitative and, in some cases, even quantitative influence of the parameters related to the discretisation. As with any other kind of simulation (e.g. fluid dynamics [4]), two major decisions have to be made for the description to be used: macro- vs. microscopic and discrete vs. continuous [5]. Although we do not consider it explicitly here, performing the continuum limit of the discrete models would contribute to a better understanding of their relation to continuous models.

As we will see, the discreteness leads to some problems that will be exemplified using the so-called floor field CA model that has been introduced in [6, 7, 8]. The big advantage of this model compared to other CA approaches for pedestrian dynamics [9, 10, 11, 12, 13] is that the floor field model is able to reproduce most of the characteristic aspects of pedestrian dynamics, especially the different collective effects observed empirically [1, 2, 14, 15]. Here, the inclusion of friction effects allows to describe many important observations, especially in egress and evacuation scenarios [8, 16].

There are foremost three basic parameters any CA model is based on: the interaction range, which in traffic models [17] usually is given by the maximal velocity v_{\max} , the time scale Δt and the generic length scale a , corresponding to the size of one grid cell. The variation of Δt will only cause the rescaling of all time values such as averaged evacuation times and is therefore from a theoretical point of view not very interesting. In contrast, variations of v_{\max} and a will turn out to have a strong qualitative influence on the *dynamical* properties of the model.

The outline of the paper is as follows: First, we present extensions of the basic model (with $v_{\max} = 1$) to larger interaction ranges $v_{\max} > 1$. Four possible variants of the extension are considered, based on different aspects of the dynamics, especially the treatment of crossing paths. Monte Carlo simulations will be presented and compared to empirical data. Then we investigate the effects of a reduction of the length scale a . We will also show that a finer spatial discretisation (by reducing a from $a = 40$ cm to $a = 20$ cm) has strong effects on the dynamics.

But first, we will review the most important characteristics of the basic model with $v_{\max} = 1$ and $a = 40$ cm in the next section.

2. Cellular automata models

For pedestrian dynamics, in a natural spatial discretization one introduces cells of $40\text{ cm} \times 40\text{ cm}$. This corresponds to the typical space occupied by a person in a dense crowd. Therefore, each cell can then either be empty or occupied by (at most) one pedestrian (hard-core exclusion).

Most CA approaches use a parallel (synchronous) update where the dynamical rules \mathcal{Z} have to be applied to all particles at the same time. This introduces a timescale Δt .

In stochastic CA models the motion to other cells at each discrete time step $t \rightarrow t + \Delta t$ is controlled by transition probabilities. In the simplest case, which is used most often, each pedestrian is allowed to move only to one of his/her four nearest neighbour cells.

The effects of the discretisation and interaction range that we want to investigate here will appear in any CA model. However, our testing ground will be a specific CA, namely the floor field model. It can be regarded as a two-dimensional generalization of the asymmetric simple exclusion process (ASEP) (see e.g. [18, 19]) where the transition probabilities are determined *dynamically* through a coupling to so-called *floor fields* [6, 7]. In turn, these floor fields are changed by the motion of the pedestrians which leads to feedback effects. This way of implementing the interactions is inspired by the form of communication in insects societies (e.g. ants) and the interaction can be described as *virtual chemotaxis*. Generically a movement in the direction of larger fields is preferred. The key point is that an interaction that is long ranged in space can be translated into a local interaction, but with “memory”. Note that in contrast to chemotaxis and trail formation [20, 21, 22, 23] in our model the trace is only virtual, i.e. can not be observed empirically. We do not give a full definition and discussion of the floor field model, which can be found in [6, 7, 8, 24, 25], but focus on the aspects that are important in the following.

The floor field consists of two parts, a static and a dynamic field. Both are discrete and we can imagine the field strength as the number of virtual pheromones present at a site. The fixed *static floor field* S is not changed by the presence of the pedestrians. S is used to specify regions of space which are more attractive, e.g. exits or shop windows. In case of an evacuation simulation the static floor field S describes the shortest distance to the closest exit door measured in steps, i.e. the number of lattice sites to the exit [7]. Steps can be carried out to the four next neighbour sites. The field values increase towards the door.

Collective effects like lane formation or herding [1, 2, 26, 27] that are based on a long range interaction between pedestrians can be taken into account by a dynamically varying floor field D [6]. The *dynamic floor field* D is a virtual trace left by the pedestrians and has its own dynamics, i.e. diffusion and decay. It is used to model different forms of interaction between the pedestrians. At $t = 0$ the dynamic field is set to zero for all sites (x, y) of the lattice, i.e. $D_{xy} = 0$. Whenever a particle jumps from site (x, y) to one of the four neighbouring cells, D at the origin cell is increased by one: $D_{xy} \rightarrow D_{xy} + 1$. Furthermore, the dynamic floor field is time dependent, it has diffusion and decay controlled by two parameters $0 \leq \alpha, \delta \leq 1$, which leads to broadening and dilution of the trace [6].

The coupling of the particles to the static and dynamic floor field is controlled by coupling constants k_S and k_D , respectively. A strong coupling to the static field implies an almost deterministic motion in the direction of larger fields. On the other hand, if the coupling to the dynamic field dominates, herding effects become important where pedestrians blindly follow others as it may happen in the case of panic.

An important extension that makes the dynamics more realistic is the concept of

friction [8, 16]. It has been implemented in other models in a direct way as contact friction [27]. However, in our approach it concerns the behavior of two (or more) pedestrians that try to move to the same cell. With some probability μ , called friction parameter, none of the particles is allowed to move, whereas with probability $1 - \mu$ one of the particles is chosen randomly to occupy the target cell. This leads to effects similar to arching in granular materials [27, 28].

3. Extensions to $v_{\max} > 1$

In the definition of the model given above, particles are only allowed to move to unoccupied *nearest* neighbour sites in one time step $t \rightarrow t + \Delta t$, i.e. $v_{\max} = 1$ cell/time step. This constraint corresponds to a maximum empirical walking speed of $v_{\text{emp}} = 1.3$ m/s [14, 15], if the time scale Δt is identified with 0.3 s. The choice $v_{\max} = 1$ has the advantage of simplicity and high simulation speed. It also reproduces most experimentally observable phenomena. Nevertheless, there are reasons for the introduction of higher walking speeds $v_{\max} > 1$ in some cases:

- (i) Fig. 1 shows the fundamental diagram of the flow along a corridor in the $v_{\max} = 1$ case of large coupling k_S and $k_D = 0$. § It is nearly symmetric with maximal flow at $\rho \approx \frac{1}{2}$. However, experimental data point to a non-symmetric fundamental diagram with maximal values of the flow for densities $\rho < \frac{1}{2}$ [14, 15].
- (ii) The interaction horizon is not isotropic since pedestrians react mainly to stimuli in front of them. This anisotropy can be better taken into account in a model with larger interaction range where it is generated dynamically through the exclusion principle.
- (iii) Although the velocity distribution of a pedestrian is sharply peaked around 1.3 m/s, higher walking speeds are frequently observed [14, 15].
- (iv) In a model with $v_{\max} > 1$, a realistic distribution of different walking speeds of the particle ensemble can be implemented in a simple way.

Certainly the most relevant aspects are the first two. The other two requirements could be taken into account in the case $v_{\max} = 1$ by introducing individual randomization probabilities, determined by the coupling constants k_S and k_D , or a rescaling of the relevant time scale. In the following extensions of the model to $v_{\max} > 1$ will be presented. The possible variants of the update algorithm and their dynamical properties will be discussed in detail and compared to experimental data.

3.1. Classification of the model variants

In the case of $v_{\max} = 1$, the particles are allowed to cover a maximal distance of $a = 40$ cm (corresponding to a movement to next neighbouring sites) per time step. Then

§ The empirical unit of the specific flow is pedestrians/(meter·second), the natural unit of the model: particles/($a \cdot \Delta t$) (with cell length $a = 40$ cm and time scale Δt).

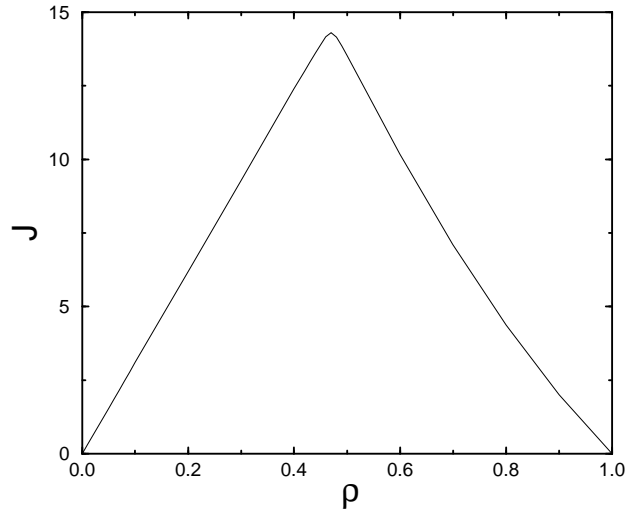


Figure 1. Fundamental diagram (flow J , measured in units of $1/\Delta t$, vs. density ρ , measured in units of $\rho_{\max} = 1/a^2 = 6.25 \text{ m}^{-2}$) for a corridor of 93×33 lattice cells of size $a^2 = 40 \times 40 \text{ cm}^2$ with $v_{\max} = 1$ in the so-called ordered regime ($k_S = 10.0$ and $k_D = 0.0$). The static floor field S is calculated using a Manhattan metric. In the direction of the flow periodic boundary conditions are used. For details see [7, 24].

for higher walking speeds $v_{\max} \geq 2$ the particles should be able to cover a distance of $v_{\max} \cdot a$ in one time step. This does not necessarily correspond to higher velocities, e.g. when combined with a reduction of the cell size or change of time scale, which is the case mainly considered here. Then, due to the two-dimensional nature of the motion, the chosen path is not necessarily straight. Also it has to be taken into account that now the paths of different pedestrians may cross. This requires a generalization of the concept of friction. In the following we develop a formalism which allows to describe the different possible generalizations.

At the beginning of a time step t the position of each particle $n \in \{1, \dots, N\}$ is denoted by $T_0^{(n)}(t)$. Each particle then chooses, corresponding to its desired movement, a trajectory $T^{(n)}(t) = \{T_0^{(n)}(t), \dots, T_{v_{\max}}^{(n)}(t)\}$ consisting of $v_{\max} + 1$ lattice sites. The single elements of $T^{(n)}(t)$ are determined by applying the update rules \mathcal{Z} for the $v_{\max} = 1$ case successively v_{\max} times. Here, every arbitrary element $T_l^{(n)}(t)$ ($l > 0$) corresponds to a target site \mathcal{Z} of the particle n that has advanced virtually to site $T_{l-1}^{(n)}(t)$ (see Fig. 2):

$$T_l^{(n)}(t) = \mathcal{Z}(T_{l-1}^{(n)}(t)). \quad (1)$$

Therefore, $T_l^{(n)}(t)$ can only be one of the four next neighbour sites of $T_{l-1}^{(n)}(t)$ or $T_l^{(n)}(t) = T_{l-1}^{(n)}(t)$. Thus, every particle accesses iteratively at most v_{\max} target sites. It is important to notice that the v_{\max} target sites and thus the trajectories are determined using the configuration of the system at time t through $\{T_0^{(1)}(t), \dots, T_0^{(N)}(t)\}$.

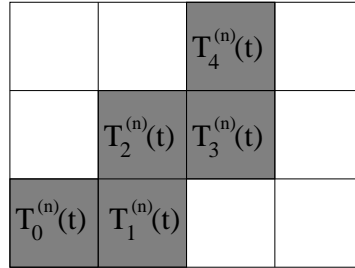


Figure 2. Graphical representation of the desired trajectory $T_l^{(n)}(t)$ of pedestrian n for the case $v_{\max} \geq 4$.

All desired trajectories can be summarized in the matrix

$$T(t) = \begin{pmatrix} T_0^{(1)}(t) & \cdots & T_{v_{\max}}^{(1)}(t) \\ \vdots & \ddots & \vdots \\ T_0^{(N)}(t) & \cdots & T_{v_{\max}}^{(N)}(t) \end{pmatrix}, \quad (2)$$

which has to be stored at every time step of the simulation. Two basic assumptions of the model are reflected by the matrix elements of $T(t)$:

- Hard-core exclusion of particles: $T_0^{(i)}(t) \neq T_0^{(j)}(t)$ for all $i \neq j$, i.e. every lattice site can be occupied by at most one particle.
- Parallel updating: $T_{v_{\max}}^{(i)}(t) \neq T_{v_{\max}}^{(j)}(t)$ for all $i \neq j$. This expresses the reaction time of the particles. No particle can occupy a lattice site at time step $t + 1$, which was occupied at time step t by another one.

These properties are special cases of the more general rule $T_n^{(i)}(t) \neq T_n^{(j)}(t)$ for all $i \neq j$ and $n = 0, 1, \dots, v_{\max}$. They restrict the allowed values of the first and last column of $T(t)$, i.e. the allowed positions at time t and $t + \Delta t$. The remaining $v_{\max} - 1$ columns correspond to intermediate states that are not explicitly realized as configurations. It might happen that two or more desired trajectories cross or that even one of the intermediate states violates the hard-core exclusion principle. In the following we will denote such situations as *conflicts*. In principle one could ignore the existence of conflicts since they correspond only to virtual intermediate states. However, in order to make the dynamics more realistic it is necessary to take them seriously. Then a method for the resolution of conflicts is required. In the following we will discuss four major variants.

3.1.1. Hop or stop The simplest variant ignores the intermediate positions $T_l^{(n)}(t)$ ($l = 1, \dots, v_{\max} - 1$) and takes only conflicts in the desired new positions $T_{v_{\max}}^{(n)}(t)$ into account. If k particles ($k \geq 2$) have chosen the same target cell, i.e.

$$T_{v_{\max}}^{(i)}(t) = T_{v_{\max}}^{(j)}(t), \quad \text{for all } i, j \in \{1, \dots, k\}, \quad (3)$$

one particle i is chosen by a probabilistic method (i.e. in random order) and is allowed to move to target site $T_{v_{\max}}^{(i)}(t) =: T_0^{(i)}(t + 1)$. The other $k - 1$ particles $j \neq i$ involved in the conflict are not allowed to move and have to remain at their origin sites, i.e.

$T_0^{(j)}(t+1) = T_0^{(j)}(t)$. Practically, this can be easily implemented by allowing all particles to move sequentially by choosing randomly a permutation σ of the particle indices j that determines the order $\sigma(j)$ of updating||.

This is the simplest form of conflict resolution between particles. The overall movement takes place without consideration of the trajectories $T^{(n)}(t)$. Crossing trajectories and jumping over already advanced particles are permitted in order to keep the spirit of the parallel updating scheme.

3.1.2. Move as far as possible This variant of conflict resolution is similar to the previous one. Again the particles are allowed to move in random order described by a randomly chosen permutation σ . However, now other particles that have already reached their target sites cannot be jumped over by following particles anymore. A particle n is able to proceed along its trajectory $T^{(n)}(t)$, as long as $T_l^{(n)}(t)$ ($l \in \{1, \dots, v_{\max}\}$) is not already occupied by another particle.

In this variant crossing trajectories are still possible, but jumps over particles that have already reached their target sites are not allowed.

3.1.3. v_{\max} sub-steps In this variant of the update the particle movement along the trajectories $T_n(t)$ is subdivided into v_{\max} sub-time steps where moves to nearest-neighbour cells are allowed. If in one sub-time step l , two or more (at most four) particles try to move to the same cell, i.e.

$$T_l^{(i)} = T_l^{(j)}, \quad \text{for any } i, j, \quad (4)$$

only one randomly chosen particle is allowed to move forward to this site. All other particles then try to reach the site during the next sub-time step $l + 1$.

In all sub-time steps of this update version conflicts between particles are taken into account and solved. Therefore, it is the easiest way to incorporate the concept of friction [8] into the model with $v_{\max} > 1$. Otherwise, this method leads to increased simulation times due to the successive treatment of the sub-time steps. Note, that the dynamics of this variant is different from the genuine $v_{\max} = 1$ -case, since the trajectories $T^{(n)}$ are fixed during the whole time step.

3.1.4. No crossing paths In this last version, no particle is allowed to cross the trajectory of a particle that has already moved. The particles move in random order. If the path of particle n crosses that of a particle n' that has already moved (i.e. $\sigma(n') < \sigma(n)$),

$$T_l^{(n)} = T_k^{(n')}, \quad \text{with } l, k \text{ arbitrary}, \quad (5)$$

then

$$T_0^{(n)}(t+1) = T_{l-1}^{(n)}(t). \quad (6)$$

|| This implies that the particles move in the order $\sigma^{-1}(1), \sigma^{-1}(2), \dots, \sigma^{-1}(N)$.

k is in this case assumed to be the smallest index in the trajectory of n' for which this condition holds. Therefore, in this variant a particle is allowed to move until it reaches a cell that is either occupied or has been passed by previous particle that has already been moved at the same time step.

3.1.5. General aspects of the variants In all variants, at the end of each time step the field values of the dynamic field D at all lattice sites of the trajectories traversed by particles are increased by one. Afterwards D is modified by its decay and diffusion dynamics as described in [6, 7].

Each of the four update versions is stressing different aspects of the two-dimensional motion on the lattice. Fig. 3 shows a representation of all different methods for conflict resolution. All four variants reduce to the basic model described in Sec. 2 in the case of

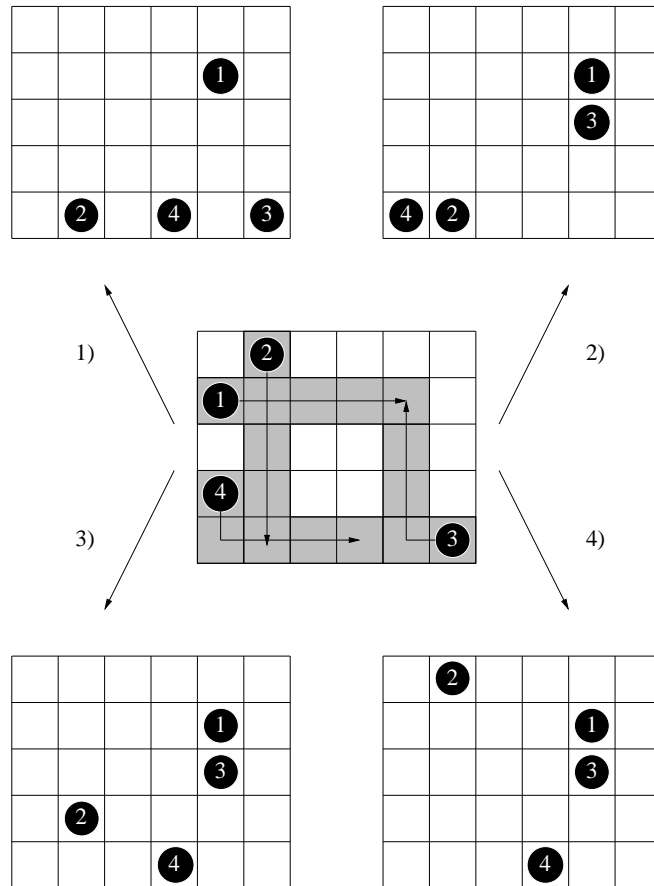


Figure 3. Graphical representation of all variants of conflict resolution in the case $v_{\max} = 4$. The trajectories $T^{(n)}(t)$ of the particles are shaded gray. The numbers of the particles correspond to the random order (given by the permutation σ) in which the particles execute their steps. In variants 1), 2) and 4) this order is designated once. In the variant 3) one has to choose a new random order in every single sub-time step.

$$v_{\max} = 1.$$

The characteristic time-scale Δt should not be influenced by the choice $v_{\max} > 1$. Therefore, for a given value of v_{\max} the corresponding maximum empirical walking speed can be calculated via

$$v_{\max}^{(\text{emp})} = v_{\max} \cdot \frac{a}{\Delta t} = v_{\max} \cdot 1.3 \text{ m/s} \quad (7)$$

with $a = 40 \text{ cm}$ and $\Delta t = 0.3 \text{ sec}$.

In the following, the consequences of higher walking speeds on particle flows will be investigated and the differences between the four variants are discussed. Afterwards, the dependence of the evacuation time for a room on v_{\max} is investigated.

3.2. Simulations

The particle flows $J = \rho \langle v_x \rangle$ presented in this section are measured in a corridor of size $X \times Y = 93 \times 33$ with periodic boundary conditions in x -direction. The motion in y -direction is limited by walls. The static floor field S increases from left to right, i.e. $S_{x,y} = x$ [16]. We remind the reader, that in the floor field model a motion in the direction of increasing field strength is preferred. The lattice was initialized by randomly distributing N pedestrians corresponding to a density $\rho = N/(X \cdot Y)$. If not stated otherwise, the coupling k_D to the dynamical field vanishes ($k_D = 0$) and therefore the dynamical parameters of D can be chosen as $\alpha = 0$ and $\delta = 1$.

3.2.1. Fundamental diagrams for different values of v_{\max} Fig. 4 shows fundamental diagrams for $v_{\max} = 1, \dots, 5$ for two of the variants discussed above. In Fig. 4a the flow

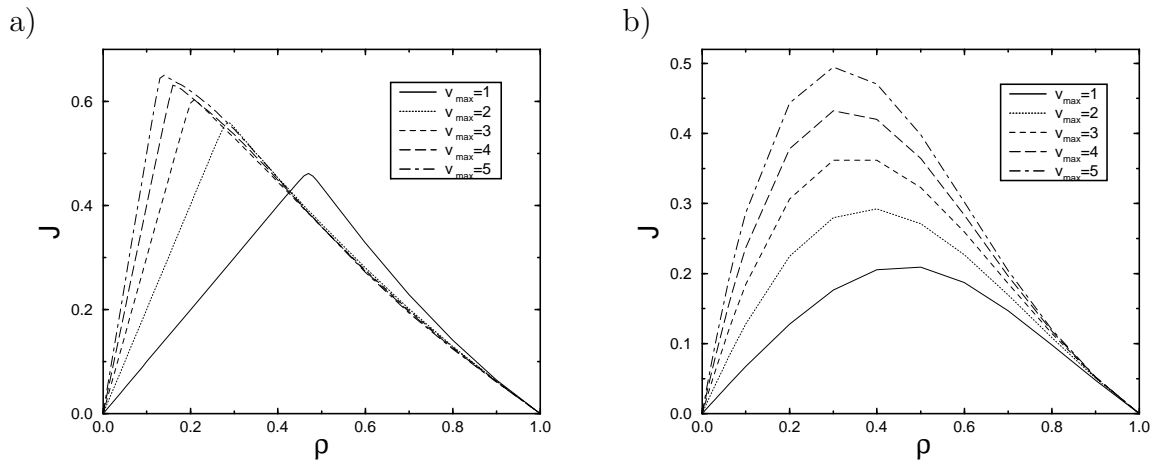


Figure 4. Fundamental diagrams for $v_{\max} = 1, \dots, 5$. **a)** Variant 4 (*no crossing paths*) with $k_S = 10.0$ and $k_D = 0.0$; **b)** Variant 2 (*move as far as possible*) with $k_S = 2.0$ and $k_D = 0.0$.

values J are shown for the case of a dominating coupling to the static field ($k_S \gg k_D$, corresponding to the ordered regime [7]). The update is based on the *no crossing paths* variant. The maximal flow is reached at smaller particle densities for growing v_{\max} . The

maximal flow is also increasing with v_{\max} . An unexpected property of this variant is that for densities $\rho > 0.4$ the flow J is largest in the case $v_{\max} = 1$. This can be explained by the blockage of wide parts of the lattice, resulting from the non-traversable trajectories of the particles. The influence of this blockage increases with v_{\max} due to an increased ‘effective density’. The faster a pedestrian moves, the more cells she or he blocks. In this respect, the *no crossing paths* scheme leads to the highest effective densities (Fig. 4).

Because of the strong coupling to the static field S , which suppresses swaying in y -direction, the fundamental diagrams look very similar to those of the ASEP or other traffic models in the deterministic limit (Fig. 4a). If one chooses, like in Fig. 4b for the second version of the update, a smaller coupling strength ($k_S = 2$), the effective walking speed v_{eff} of the particles is decreasing. For $k_S \rightarrow \infty$ the effective walking speed of a single pedestrian is $v_{\text{eff}} \rightarrow v_{\max}$, corresponding to a deterministic motion. On the other hand, for $k_S = 0$ the particle performs an isotropic random walk since the information about the preferred direction through the static floor field is not taken into account. Therefore, for $k_S = 2.0$ the shape of the fundamental diagrams is becoming smoother (Fig. 4b). The maximal values of J are smaller with a slight shift of the maximum to higher densities (for $v_{\max} > 1$) and the slopes in the regions of small and high densities decrease.

In the following, the consequences of the different conflict resolution schemes on the flow are discussed. Fig. 5 shows the fundamental diagrams of all four variants for the velocities $v_{\max} = 2$ and $v_{\max} = 4$ and $k_S = 2.0$. For $v_{\max} = 2$ the differences between the

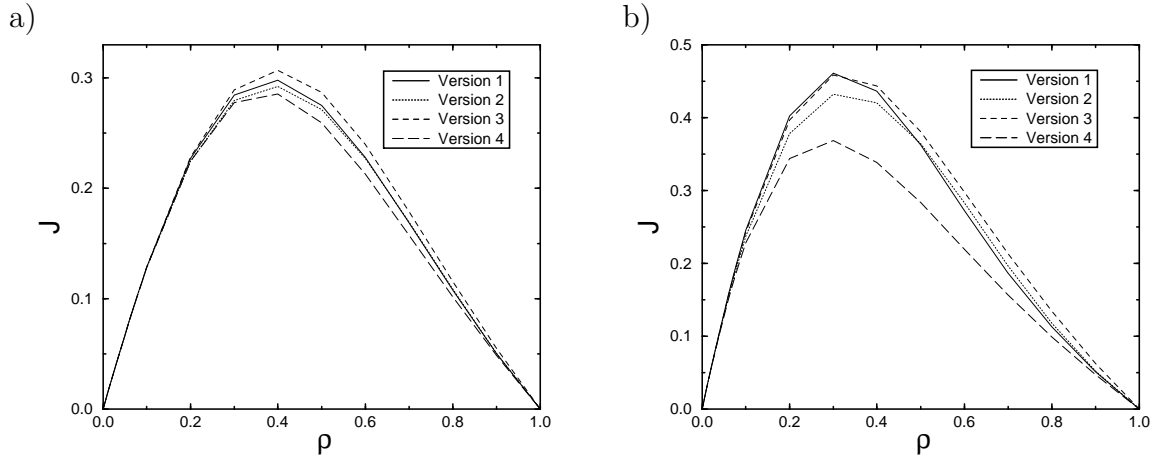


Figure 5. Fundamental diagrams for all four update variants with $k_S = 2.0$ and $k_D = 0.0$: **a)** $v_{\max} = 2$; **b)** $v_{\max} = 4$.

variants are not strongly pronounced (Fig. 5a). But the flow values J are highest for the v_{\max} *sub-steps* and smallest for the *no crossing paths* scheme in all density regions.

However, for $v_{\max} = 4$ the differences between the variants are easy to spot. For particle densities $\rho > 0.1$ the *no crossing paths* scheme produces much smaller flow values than all other variants, because of the non-traversable trajectories which are four

sites long. The third version of the update (*sub-steps*) leads to the highest flows in all density regions since the resolution of conflicts in sub-time steps enables some particles to move forward in a later sub-time step.

Finally, we compare the simulation results with empirical data. Fig. 6 shows a comparison of fundamental diagrams of the v_{\max} *sub-steps* variant (see Sec. 3.1.3) with a fit of empirical flow-density relations [14]. The data for the specific flow has been transformed to the units of the model. The fundamental diagram for $v_{\max} = 3$ is in

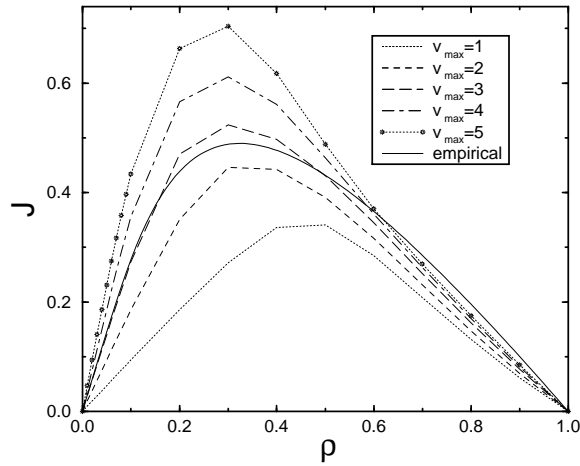


Figure 6. Comparison of fundamental diagrams of the third update version and the velocities $v_{\max} = 1$ to $v_{\max} = 5$ with experimental data from [14] ($k_S = 4.0$ and $k_D = 0.0$).

good agreement with the experimental data. In particular, the density values for the highest flow match each other very well. Since $k_S = 4.0$, the particles have a reduced effective walking speed $v_{\text{eff}} < v_{\max}$. In the model, this results in a diversification of the flows for particle velocities between $v_{\max} = 3$ and lower values. For high density regions $\rho > 0.6$ the model yields flow values which are too small. The reason are lane changes of particles especially at higher densities. If the site in front of a particle is occupied, lane changes are possible. Such a changing does not increase the flow in positive x -direction, but often inhibits the movement of another particle (see Fig. 7). The fundamental

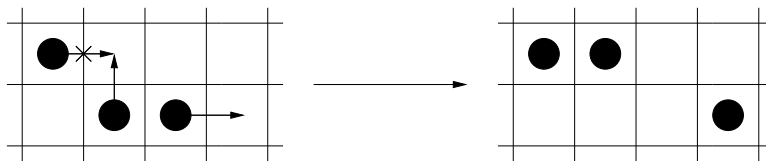


Figure 7. Decrease of the flow due to lane changes.

diagrams of the other v_{\max} values do not agree as well with the empirical data.

3.3. Simulation of the evacuation of a room

As a second scenario which helps to understand the effects of $v_{\max} > 1$ we investigate its influence on evacuation times. The room to be evacuated is a square of 63×63 cells. The exit has a width of one cell and is located at the center of one wall. Initially the particles are distributed randomly and then try to leave the room due to the information they get through the floor fields. This scenario has been studied in detail in [7] where three different regimes (*ordered* for $k_S \gg k_D$, *disordered* for $k_D \gg k_S$, and *cooperative*) have been identified.

Fig. 8 shows averaged evacuation times for different combinations of the coupling parameters k_S and k_D for the *move as far as possible* variant of the update. All other schemes show the same qualitative behaviour. The particle velocities are $v_{\max} = 1, \dots, 4$. Fig. 8a can be interpreted in the following way: If the coupling strength to the static

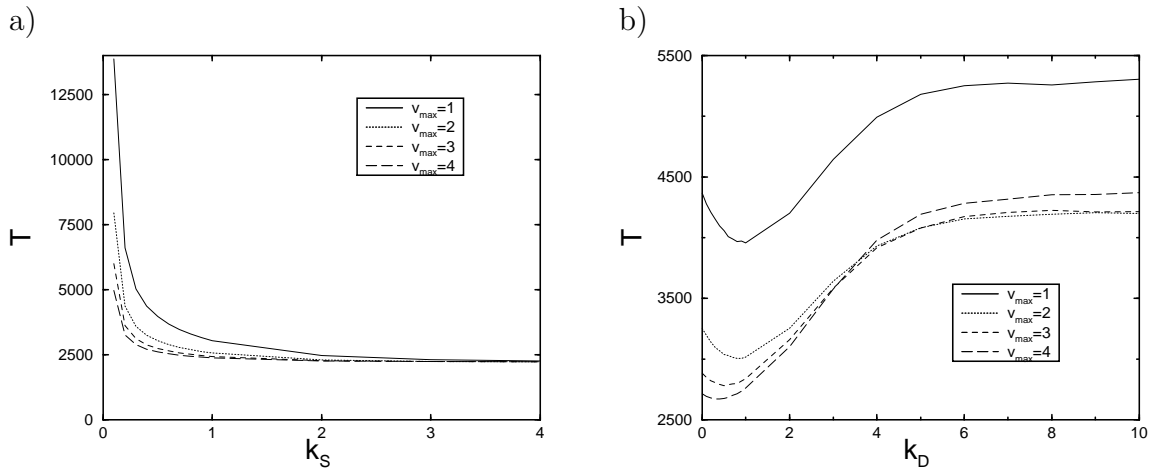


Figure 8. Averaged evacuation times for a room of size 63×63 sites and an exit of one cell. The particle density at the beginning of the evacuation is $\rho = 0.3$ (1116 randomly distributed particles). Different v_{\max} -values in the second version of the update (*move as far as possible*). **a)** $k_D = 0.0$; **b)** $k_S = 0.4$ and $\delta = 0.3$ and $\alpha = 0.0$ as parameters for the dynamics of D .

field S is very small ($k_S \ll 1$), the particle motion resembles a random walk. But even if there is only slightly directed movement, the variance in lateral direction is increased with v_{\max} . Therefore, the particles can reach the exit by chance faster for increased v_{\max} , resulting in decreased evacuation times. In the limit $k_S \rightarrow \infty$ the particles move on the shortest possible way to the exit, the movement becomes deterministic. For higher particle densities just after the evacuation starts a big jam forms in front of the exit. Therefore, the averaged evacuation times are in this case determined by the particle number (via the flow through the door) rather than the maximum walking speed. Thus, for higher densities and $k_S \rightarrow \infty$ the evacuation times using the *move as far as possible* strategy (see Fig. 8 top) are the same for all v_{\max} values.

A coupling strength of $k_S \gg 1$ is presumably most relevant for a comparison with

real pedestrian behaviour. Therefore, for many applications the restriction to $v_{\max} = 1$ is adequate to reproduce realistic behaviour. In other cases (see above) a choice of $v_{\max} > 1$ is indispensable.

Finally, Fig. 8b shows the different evacuation times for $k_D = 0.0$ and varying v_{\max} . Since k_S is very small ($k_S = 0.4$), they are decreasing with v_{\max} . The characteristic non-monotonous behaviour for increasing k_D (see [7]) is reproduced for all v_{\max} values. Since in this parameter regime the particle density is a restricting factor for the evacuation time due to the clogging occurring at the exit, for $v_{\max} \geq 2$ one finds some kind of convergence of the time values.

4. Finer discretisation of space

Increasing the maximal velocity of pedestrians is not the only modification that influences the realism of the model. One of the boldest assumptions in CA models for pedestrian motion is the representation of space as a grid of cells and the corresponding restriction of the spatial resolution to the cell size, in this case 40 cm. However, it can be argued that this simplification is justified by the reaction time (or decision time) which can be easily identified in the model. Nevertheless, an – preferably qualitative – investigation of the discretization effects would shed some light on the issue. The space discretisation used so far has been chosen in the simplest possible way such that a pedestrian occupies only one cell. This leads to a length scale of $a = 40$ cm (see Sec. 2). However, for some applications this might not be adequate and a finer discretisation is necessary. In the following we will discuss the necessity of a smaller length scale, ways of its implementation and the consequences for the behaviour of the model.

4.1. Motivation and consequences

The identification of the size of one lattice site with the typical space occupied by a pedestrian in a dense crowd is most natural for the construction of a CA model for pedestrian dynamics. For square cells this leads to a cell size of $a^2 = 1/\rho_{\max}^{(\text{emp})}$ and $a = 40$ cm where $\rho_{\max}^{(\text{emp})} \approx 6.25$ persons/m² is the maximal empirically observed density [14]. All units of space are then a multiple of the length scale $a = 40$ cm. In contrast to the introduction of higher velocities discussed in the previous section which was motivated by the unrealistic shape of the fundamental diagram, there are no simulation results that indicate the necessity of a better spatial resolution. Nevertheless there are good reasons to introduce a finer discretisation of space.

- (i) If the model is used not only for basic investigations of pedestrian dynamics, but also for the assessment of evacuation scenarios in complex structures (like passenger vessels or football stadiums), an accurate representation of the geometries is desirable. A finer discretisation corresponds to a more accurate representation of geometrical structures in a natural way. This can be seen from Fig. 9.

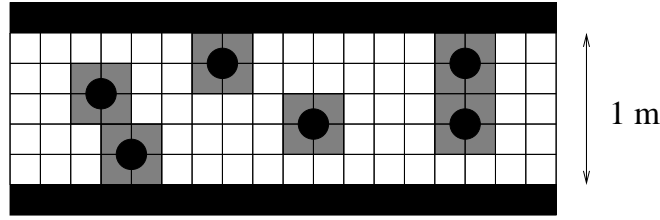


Figure 9. Representation of a corridor of width 1 m in the 20-cm-model. Such a corridor can not be reproduced exactly in the 40-cm-model. The four cells occupied by each particle are shaded gray.

- (ii) As we have seen in Sec. 3 some situations require the use of higher velocities $v_{\max} > 1$. If one wants to keep the time scale unchanged this has to be compensated by introducing a smaller length scale.
- (iii) In principle it would be interesting to consider the continuum limit $a \rightarrow 0$ in order to make contact with models that are based on a continuous representation of space, e.g. the social force [26, 29] and similar models [30] or hydrodynamic approaches [31, 32, 33, 34, 35].

The straightforward approach to investigate the discretization effects is to vary the cell size. If one chooses a cell size of $a = 20$ cm, the area $A = 1/\rho_{\max}^{(\text{emp})}$ occupied by a pedestrian is 4 cells (see Fig. 9) in order to reproduce the maximal density $\rho_{\max}^{(\text{emp})}$. The natural generalisation for the allowed motion of the original model as described in Sec. 2 (in the following denoted as 40-cm-model) is the motion of the center of a pedestrian by one cell (i.e. a distance a , see Fig. 10). This is only possible if the two neighbouring cells are unoccupied. As can be seen from the relation (7) (with $v_{\max} = 1$) for the three fundamental quantities the time step Δt in the 20-cm-model is half as long as in the 40-cm-model¶. For the empirical velocity of $v_{\text{emp}} = 1.3$ m/s and $a = 20$ cm the time scale is $\Delta t = 0.15$ sec. For an arbitrary spatial discretisation a one obtains the time scale $\Delta t = a/v_{\max}^{(\text{emp})}$.

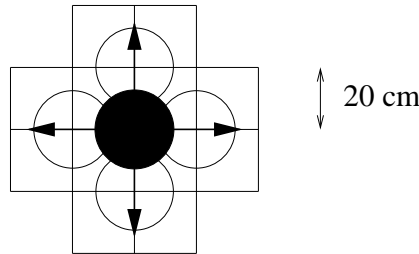


Figure 10. Occupation of 2×2 lattice sites of cell length $a = 20$ cm and possible transitions in a time step.

¶ An extension of the 20-cm-model to a model with walking speeds $v_{\max} > 1$ is possible in the same way as discussed in the previous section, but will not be considered in the following.

Finer discretisations of the underlying geometric structure for fixed velocity v_{\max} therefore lead to smaller length and time scales of the model. So the limit $a \rightarrow 0$ results in a space *and* time continuous model. This limit allows a comparison between discrete and continuous models, but is not considered here.

The occupation of four lattice sites by one particle has further consequences in the 20-cm-model, especially for the floor field model described in Sec. 2.

- (i) Every particle leaves two of the four cells it occupied previously (Fig. 10). In both these cells the dynamic floor field has to be increased.
- (ii) Since a particle occupies always four lattice sites, the transition probabilities are calculated by averaging the specific field values of static and dynamic floor fields S and D .

In any CA, not only the floor field model, an important new effect related to conflicts occurs when the cell size is reduced and particles occupy more than just one cell. In the 40-cm-model, conflicts can be described as *local* interactions (Fig. 11a), because only a small number of particles can access the same lattice site which is determined by the coordination number of the lattice. On the other hand, in the 20-cm-model conflicts are not necessarily local anymore. Here, conflicts are not restricted to single cells and can spread over a wider area of the lattice. This is illustrated for a typical situation in Fig. 11b. Assume that the permutation σ (see Sec. 3.1.1) is such that the particles move from “left to right”, i.e. all the particles in the top row are allowed to move and the particles in the bottom row are not. Switching $\sigma^{-1}(1)$ and $\sigma^{-1}(2)$ will change the movement of all particles. This is not the case for particles that occupy only one cell, i.e. $a = 40$ cm.

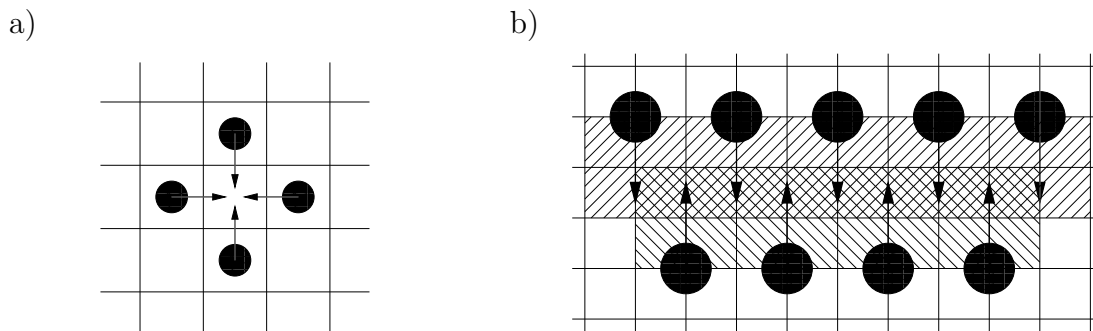


Figure 11. a) Typical local conflict in the 40-cm-model. b) In the 20-cm-model in principle all particles of a system can be part of a conflict. Hatched cells contribute to the non-local conflict.

In the floor field model conflicts allow for the introduction of friction parameter μ [8, 16] (see Sec. 2). Due to the possible non-local nature of conflicts in the 20-cm-model this concept can not straightforwardly be generalized. New concepts for the description of conflicts are necessary, which is currently under investigation and will be discussed in a future publication.

In the next section simulation results of the 20-cm-model will be compared to results of the conventional model.

4.2. Simulation results

4.2.1. Evacuation times First, we will turn to the influence of the discretisation on evacuation times. We measured the averaged times of the evacuation of a large single room with an area of about $(24.8 \text{ m})^2$, corresponding to 62×62 cells for the $a = 40$ -cm-model or 124×124 cells for the $a = 20$ -cm-model. The particles leave the room via a door of width 80 cm (two or four lattice sites, respectively). Fig. 12 shows the impact of the variation of the parameters k_S and k_D in the $a = 20$ -cm and $a = 40$ -cm-model⁺. The initial particle density is $\rho = 0.3$ corresponding to 1153 particles. The qualitative

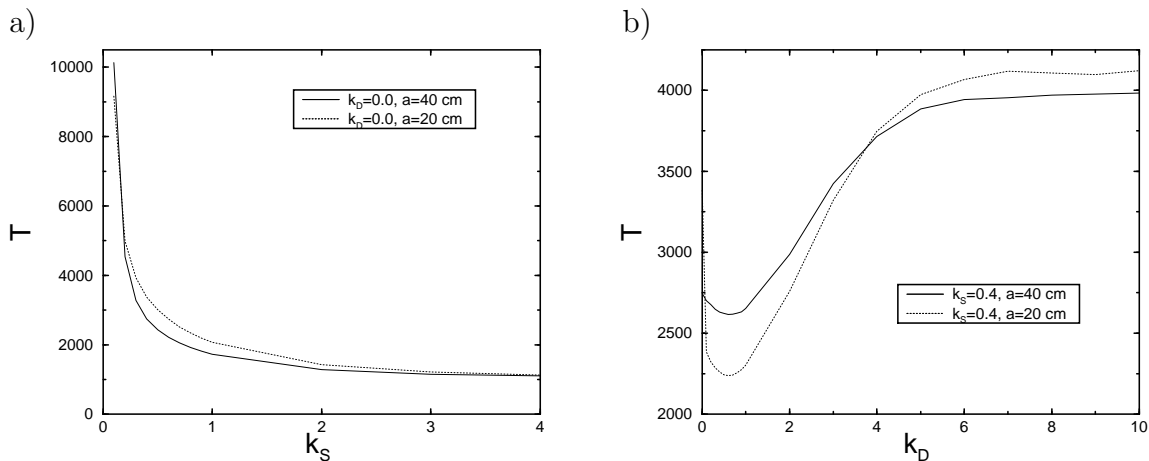


Figure 12. Averaged evacuation times for a room of size $62 \cdot 40 \text{ cm} \times 62 \cdot 40 \text{ cm}$ and an exit of width 80 cm: **a)** $k_D = 0.0$ fixed and variation of k_S ; **b)** $k_S = 0.4$ fixed and variation of k_D ($\delta = 0.3$ and $\alpha = 0.0$).

behaviour of the model when varying the parameters (see Sec. 3 and [7]) is not influenced by the finer discretisation. Because of slightly different transition probabilities due to the averaging of the field values of four sites for each walking direction in the $a = 20$ -cm-model, small deviations only exist for coupling strengths $k_S < 3$ (see Fig. 12a). This also leads to different time values for the parameter choice $k_D = 0.0$ and $k_S = 0.4$ in Fig. 12b). It is remarkable that the effect of the non-monotonic parameter dependence [7] of the curve is most pronounced in the $a = 20$ -cm-model.

The most important difference between the 20 cm- and 40 cm-model is the possibility of a deadlock in front of a small exit. Consider the flow through a bottleneck of the dimension of the particle width (i.e. bottleneck and particle have the width of two cells or 40 cm). If two particles reach the bottleneck at the same time step, their

⁺ The times are measured in update steps. Therefore, for a comparison of the two models, the simulation times of the $a = 20$ -cm-model have to be divided by two.

mutual blockage (see Fig. 13) may lead to vanishing flows. Similar observations have been reported in experimental investigations (see e.g. [36, 37]). This phenomenon can

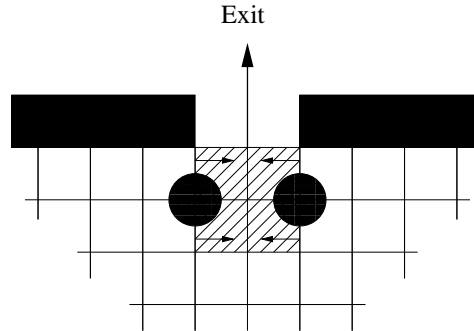


Figure 13. Blockage of bottlenecks or exits of width 40 cm in the 20-cm-model caused by two particles. Both particles try to access the four lattice sites in front of the exit.

occur in pushing pedestrian crowds at bottleneck-shaped exits of small width. It has also been observed for some continuum pedestrian models with extended particles [27] and similarly in granular flow through a funnel [38, 39]. Therefore it is remarkable that it does *not* appear in the original 40-cm-model.

On the other hand, the movement itself is more effective for the 20 cm-model compared to the 40 cm-model. For very high values of k_S , the overall evacuation time is determined by the outflow through the door. In the case considered here ($w = 80 \text{ cm} = 4$ cells if $a = 20 \text{ cm}$), the blockage does basically not occur. For very low values of k_S (cf. Fig. 12), the particles perform a random walk and therefore the discretization ($a = 20 \text{ cm}$ vs. $a = 40 \text{ cm}$) does not play a prominent role. This interpretation is also supported by the results shown in Fig. 15 where the smallest possible exit is investigated. In this case, the flow increases with the density for small coupling strengths k_S and increases with large coupling strengths. However, this does not really explain the subtle differences in the area $0.5 \leq k_S \leq 2$, which will be investigated in more detail at a later point.

4.2.2. Flow measurements The discretisation has a significant influence on the flow. Fig. 14 shows the fundamental diagrams in the ordered regime for a corridor of width 2 m (i.e. width five lattice sites in the $a = 40\text{-cm}$ -model and ten lattice sites in the $a = 20\text{-cm}$ -model). The flows of both models are identical up to $\rho \approx \frac{1}{2}$. The density region $\rho < \frac{1}{2}$ characterises in both models the free flow regime. Nearly all particles can move to their right next neighbour site in each time step, the flow increases linearly with the density. For a density of $\rho \approx \frac{1}{2}$, the probability of occupied next neighbour sites is highly increasing in the 40-cm-model, so the average velocity of the particles is decreasing to a value $\langle v_x \rangle < 1$. Therefore, the flow decreases with increasing density and is additionally decreased by lane changing events (see Fig. 7).

The behaviour is different in the 20-cm-model: The space a particle needs for unimpeded movement in one time step corresponds to only half the length of its own

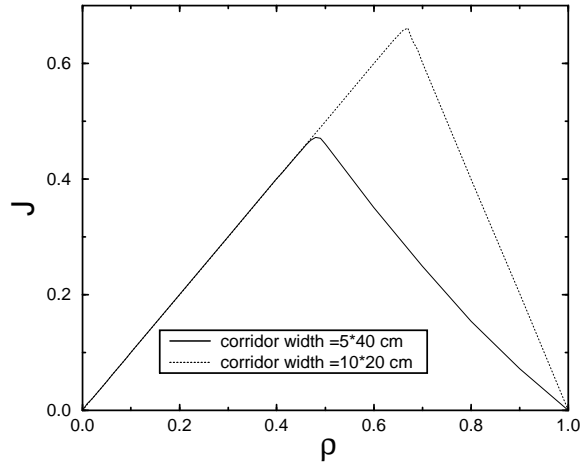


Figure 14. Fundamental diagrams in the ordered regime ($k_S = 10.0$, $k_D = 0.0$) of both model variants. Width of corridor: 5 cells in the 40-cm-model and 10 cells in the 20-cm-model.

size. Therefore, the average particle velocity is $\langle v_x \rangle \approx 1$ up to a density of $\rho \approx \frac{2}{3}$, which leads to a linear increase of the flow up to this density. For $\rho > \frac{2}{3}$ one finds a sharp decrease of the flow.

Thus the finer discretisation results in a shift of the maximum flow to regions of higher density. This effect will be present for even finer discretisations. As in Sec. 3, experimental data point at a realistic flow maximum for densities $\rho < \frac{1}{2}$. Therefore the 20-cm-model (with $v_{\max} = 1$) can not reproduce these results qualitatively.

Fig. 15 shows the flow J through a bottleneck of width 40 cm versus the parameters k_S and ρ . Only for very small k_S ($k_S = 0.1$) a small particle flow is sustained for higher densities. For increasing k_S the flow breaks down at very small densities (for $k_S = 10.0$ the flow is zero for all densities). The system freezes for growing coupling strength k_S to the static floor field. This is somewhat similar to the paradoxical *faster-is-slower-effect* [2, 27], as an increasing k_S implies higher individual walking speeds. The clogging effect observed in our model is due to the local blockage shown in Fig. 13.

5. Conclusion

We have systematically investigated the influence of the interaction range v_{\max} and the spatial discretisation a on the behaviour of two-dimensional CA models for pedestrian motion. Using simulations of a corridor and evacuation from a large room we have shown that both parameters can have a significant influence on the properties of the model. Although we have used a specific model, the floor field CA, for our simulations due to its ability to reproduce the observed *collective* phenomena correctly we believe that the effects discussed here are generic for any discrete approach to pedestrian dynamics. Of

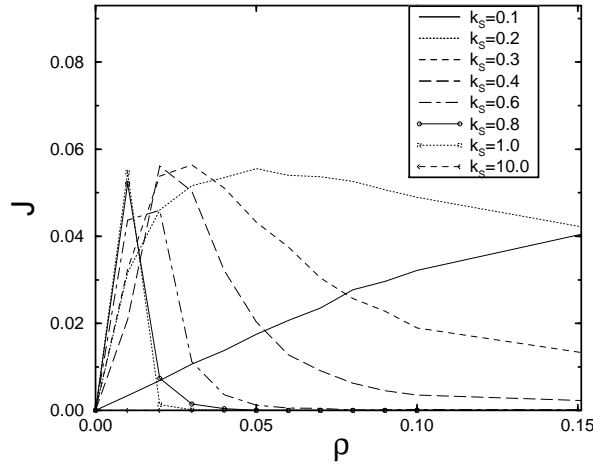


Figure 15. Fundamental diagram of a corridor (93×33 cells of size $40 \text{ cm} \times 40 \text{ cm}$) with a bottleneck of width 40 cm . The couplings to the static and dynamic floor fields are k_S and $k_D = 0.0$.

course this requires further investigations in the future.

First we have considered the extension of the interaction range which we have implemented through a larger walking speed v_{\max} . We have seen that there are different possibilities to achieve this. This modification leads to a considerable improvement of the agreement of fundamental diagrams for the motion along a corridor with empirical findings. In the original case $v_{\max} = 1$ the fundamental diagram of the model was almost symmetric with respect to the density $\rho = 0.5$. The reason is that for a such a uni-directional motion where swaying is strongly suppressed many models effectively reduce to a number of independent ASEPs* and hence the observed flow-density relation reflects its particle-hole symmetry. As in models of highway traffic [17] the maximum in the homogeneous case is shifted to lower densities for larger $v_{\max} = 2$ and thus leads to a more realistic approach.

As a second scenario we have studied the evacuation from a large room. Here it turned out that in most cases the results are not affected strongly by the introduction of a larger velocity v_{\max} .

Summarizing, these results indicate that the choice $v_{\max} = 1$ might not in all cases be justified. As indicated above the fact that for the corridor one has to deal with a basically one-dimensional motion is important. Here it is remarkable that also for a continuum model like the social force model this problem requires a rather different choice of interaction parameters [37] compared e.g. to evacuation problems, especially concerning the repulsive interaction forces. This shows that both model classes have to be generalized in order to achieve a proper description of all possible situations in a

* One could expect that in the case of a mixture of species with different v_{\max} the decoupling of the lanes will be less pronounced.

unified way.

The case of the second non-trivial fundamental parameter, namely the cell size, is even more intricate. A finer spatial discretisation does not only provide a connection to a different class of microscopic models based on continuous representation of space. In many applications to real life problems the geometries under consideration can not be described by lengths that are multiples of the length scale $a = 40$ cm of the original model. We have argued that a reduction of this length scale, and thus the cell size, must be accompanied by an increase of the size of the particles. In order to reproduce the empirically observed maximal density they have to occupy now more than one cell, e.g. four in the case of $a = 20$ cm. If the particles should have the same symmetry as the underlying lattice this also restricts the allowed length scales. E.g. for the square lattice the most natural extensions of the particles are $2^n \times 2^n$ cells corresponding to a length scale $a_n = \frac{40}{n}$ cm.

By studying the same two scenarios as for the influence of v_{\max} we found two main consequences of using a finer discretisation. On the one hand, the flow is increased since the particles can now move ahead if there is space available less than their own size. On the other hand, particles can now block each other more easily. This might lead to non-local conflicts where groups of pedestrians mutually block each others motion (Fig. 11). Furthermore, at exits blocking can result in a complete breakdown of the outflow. This is not related to the discreteness of the model and can also be observed in continuum models with particles of finite size.

It would be interesting to perform the continuum limit of our model to relate it to other continuum approaches. A naive continuum version of the floor field model is currently under investigation and might serve as a reference model. Our present study has shown that finer discretisation or larger velocities in combination with a discrete time (parallel) dynamics leads to the possibility of complicated conflict situations. One could try to solve this problem by using a continuous time dynamics, but this might drastically increase the computational complexity of the model in a different way.

Even though our investigations are based on a square grid (one could also think of a hexagonal lattice, and indeed there are models based on this [40, 41]) the results obtained are generally valid. As a next step currently the combined effect of larger v_{\max} and smaller cells is investigated. Then one can expect to encounter a combination of many effects observed here. However, e.g. in the case of flow along a corridor these modifications have opposite quantitative effects. Whereas an increase of v_{\max} tends to shift the location of maximal flow to smaller densities the reduction of the length scale has the opposite effect. This work is in progress and will be reported elsewhere.

Summarizing we can say that discrete models like cellular automata yield quite realistic results. E.g. the floor field model is able to reproduce collective effects (such as lane formation in counterflow etc.) observed empirically. However, for applications where also a reliable *quantitative* prediction should be made one has to take some care in the choice of the basic parameters as cell size and interaction range.

References

- [1] M. Schreckenberg and S.D. Sharma (Ed.): *Pedestrian and Evacuation Dynamics*, (Springer 2001)
- [2] D. Helbing: *Rev. Mod. Phys.* **73**, 1067 (2001)
- [3] T. Nagatani: *Rep. Prog. Phys.* **65**, 1331 (2002)
- [4] D.H. Rothman and S. Zaleski: *Lattice-Gas Cellular Automata*, (Cambridge University Press, 1997)
- [5] N. Gershenfeld: *The Nature of Mathematical Modeling*, (Cambridge University Press, 1999)
- [6] C. Burstedde, K. Klauck, A. Schadschneider, and J. Zittartz: *Physica* **A295**, 507 (2001)
- [7] A. Kirchner and A. Schadschneider: *Physica* **A312**, 260 (2002)
- [8] A. Kirchner, K. Nishinari, and A. Schadschneider: *Phys. Rev.* **E67**, 056122 (2003)
- [9] P.G. Gipps and B. Marksjö: *Math. Comp. Simul.* **27**, 95 (1985)
- [10] V. Blue and J. Adler: *Transportation Research Records* **1644**, 29 (1998)
- [11] M. Fukui and Y. Ishibashi: *J. Phys. Soc. Jpn.* **68**, 2861 (1999)
- [12] M. Muramatsu, T. Irie, and T. Nagatani: *Physica* **A267**, 487 (1999)
- [13] H. Klüpfel, T. Meyer-König, J. Wahle, and M. Schreckenberg: In *Proc. Fourth Int. Conf. on Cellular Automata for Research and Industry*, pages 63–71, (Springer, London, 2000)
- [14] U. Weidmann: *Schriftenreihe des IVT* **90**, ETH Zürich (1992)
- [15] *Special Report 209: Highway Capacity Manual*, Transportation Research Board, National Research Council, Washington, D.C., Chapter 13 (1994)
- [16] A. Kirchner, H. Klüpfel, K. Nishinari, A. Schadschneider, and M. Schreckenberg: *Physica* **A324**, 689 (2003)
- [17] D. Chowdhury, L. Santen, and A. Schadschneider: *Phys. Rep.* **329**, 199 (2000)
- [18] G.M. Schütz: *Exactly Solvable Models for Many-Body Systems*, in C. Domb and J.L. Lebowitz (eds.), *Phase Transitions and Critical Phenomena*, Vol. 19 (Academic Press, 2001)
- [19] M.R. Evans and R.A. Blythe: *Physica* **A313**, 110 (2002)
- [20] E. Ben-Jacob: *Contemp. Phys.* **34**, 247 (1993)
- [21] D. Chowdhury, V. Guttal, K. Nishinari, and A. Schadschneider: *J. Phys.* **A35**, L573 (2002)
- [22] D. Helbing, F. Schweitzer, J. Keltsch, and P. Molnar: *Phys. Rev.* **E56**, 2527 (1997)
- [23] D. Helbing, J. Keltsch, and P. Molnar: *Nature* **388**, 47 (1997)
- [24] A. Kirchner: *Dissertation, Universität zu Köln* (2002)
- [25] H. Klüpfel: *Dissertation, Universität Duisburg* (2003) (available from <http://deposit.ddb.de/cgi-bin/dokserv?idn=96883180x>)
- [26] D. Helbing and P. Molnar: *Phys. Rev.* **51**, 4282 (1995)
- [27] D. Helbing, I. Farkas, and T. Vicsek: *Nature* **407**, 487 (2000)
- [28] D.E. Wolf and P. Grassberger (Editors): *Friction, Arching, Contact Dynamics*, (World Scientific, 1997)
- [29] D. Helbing: *Behavioral Science* **36**, 298 (1991)
- [30] P. Thompson and E. Marchant: *Fire Safety Journal* **24**, 131 (1995)
- [31] L.F. Henderson: *Transp. Res.* **8**, 509 (1974)
- [32] P. DiNenno (Ed.): *SFPE Handbook of Fire Protection Engineering (2nd ed.)*, National Fire Protection Association (1995)
- [33] D. Helbing: *Complex Systems* **6**, 391 (1992)
- [34] R. Hughes: *Math. Comp. Simul.* **53**, 367 (2000)
- [35] R. Hughes: *Transp. Res. B* **36**, 507 (2001)
- [36] H. Muir, D.M. Bottomley, and C. Marrison: *Int. J. Aviat. Psych* **6**, 57 (1996)
- [37] D. Helbing, L. Buzna, and T. Werner: *Self-organized pedestrian crowd dynamics and design solutions*, [trafficforum/03120401](http://trafficforum.org/03120401) (available from www.trafficforum.org)
- [38] S. Horlück and P. Dimon: *Phys. Rev.* **E60**, 671 (1999)
- [39] S.S. Manna and H.J. Herrmann: *Eur. Phys. J.* **E1**, 341 (2000)
- [40] S. Marconi and B. Chopard: In *Cellular Automata*, *Lect. Notes Comp. Sc.* **2493**, 231 (2002) (Springer: Berlin, Heidelberg)

Discretisation effects and the influence of walking speed in cellular automata models for pedestrian dynamics

[41] S. Maniccam: *Physica* **A321**, 653 (2003)